

PCCP

Accepted Manuscript



This is an *Accepted Manuscript*, which has been through the Royal Society of Chemistry peer review process and has been accepted for publication.

Accepted Manuscripts are published online shortly after acceptance, before technical editing, formatting and proof reading. Using this free service, authors can make their results available to the community, in citable form, before we publish the edited article. We will replace this *Accepted Manuscript* with the edited and formatted *Advance Article* as soon as it is available.

You can find more information about *Accepted Manuscripts* in the [Information for Authors](#).

Please note that technical editing may introduce minor changes to the text and/or graphics, which may alter content. The journal's standard [Terms & Conditions](#) and the [Ethical guidelines](#) still apply. In no event shall the Royal Society of Chemistry be held responsible for any errors or omissions in this *Accepted Manuscript* or any consequences arising from the use of any information it contains.

Relaxation dynamics of deeply supercooled confined water in L,L-diphenylalanine micro/nanotubes[†]

P.M.G.L. Ferreira, M. Ishikawa, S. Kogikoski Jr., W. A. Alves and H. Martinho*

Received Xth XXXXXXXXXXXX 20XX, Accepted Xth XXXXXXXXXXXX 20XX

First published on the web Xth XXXXXXXXXXXX 200X

DOI: 10.1039/b000000x

The temperature dependence (10 – 290 K) of the low-frequency (20 – 150 cm⁻¹) Raman-active phonon modes of deeply supercooled confined water in L,L-diphenylalanine micro/nanotubes was analyzed. The isolated dynamics of a specific geometry of water cluster (pentamer) in supercooled confined regime was studied in detail. A fragile-to-strong transition at 204 K was observed and related to the crossing of the Widom line. Analysis of peptide vibrational modes coupled to water hydrogen bonds indicated that hydrogen bond fluctuations play an irrelevant role in this system. Our results are in agreement with the second critical point of water existence hypothesis.

1 Introduction

The distinction between gas and liquid disappears above its critical point. At pressure and temperature above this point, the system is said to be in a fluid state (supercritical fluid)¹. Supercritical fluids are recognized as possessing unique solvation properties that make them important technological materials¹. Of particular interest is the behavior of water in confined spaces. It plays a key role in protein hydration since nanoscale fluctuations associated with the so-called Widom line can influence biological processes^{2,3}.

Poole *et al.*⁴ presented a thermodynamically consistent molecular dynamical simulation study regarding the global phase behavior of supercooled water. According to these authors, in the supercooled region just below the line of homogeneous ice nucleation, a critical point of liquid-liquid coexistence (LLCP) could exist that would eliminate the first-order transition line between low-density liquid (LDL) and high-density liquid (HDL) aqueous phases. Thus, liquid-liquid phase separation and the existence of the LLCP in water remains as a plausible hypothesis and requires further verification⁵. The Widom line $T_W(P)$ corresponds to the loci of max-

ima of thermodynamic response function in the one-phase region beyond the LLCPP proposed to exist in supercooled liquid water⁴.

Molecular dynamics simulations of the TIP4P/2005 model of water performed by Kumar *et al.*⁶ indicated that the onset of the boson peak in supercooled bulk water coincides with the crossover to a predominantly LDL-like below T_W . Gallo, Corradini and Roveri⁷ studied the dynamical properties of aqueous solution of NaCl upon supercooling by molecular simulations. They found a fragile (super-Arrhenius) to a strong (Arrhenius) crossover (FSC) upon crossing the $T_W(P)$ by both ionic solution and bulk water. The FSC phenomena was theoretically predicted to occur in water at ~ 228 K⁸.

Experiments in the supercooling region are difficult to perform due to crystal nucleation processes. Thus experimental pieces of evidence concerning the different hypotheses supporting the existence of LLCPP are hard to test⁹.

In confinement, water can be more easily supercooled and studied in region of phase space where crystallization of bulk water cannot be avoided. Confined water in nanoporous silica have been extensively studied¹⁰⁻¹⁵. Faraone *et al.*¹⁰ confined water in synthesized nanoporous silica matrices MCM-41-S (pore diameters of 18 and 14 Å) and interpreted the abrupt change of the relaxation time behavior observed by quasielastic neutron scattering at $T \sim 225$ K as the predicted fragile-to-strong liquid-liquid transition. Similar findings were reported by others (see, e.g.,^{11,12}). Liu *et al.*¹³ studied water confinement in MCM-41-S as function of pressure. They found that the transition temperature decreases steadily with an increasing pressure, until it intersects the homogenous nucleation temperature line of bulk water at a pressure of 1.6 kbar. Above this pressure, it was no longer possible to discern the characteristic feature of the fragile-to-strong transition and it was elaborated that this point could be the possible second critical point of water. Later, comments on letter of Liu *et al.*¹³ were published^{16,17}. Cervený *et al.*¹⁶ argued that when confinement takes place, it occurs a change in the relaxation process that leads to a dynamic crossover from non-Arrhenius to Arrhenius behavior. This change is due to the onset of finite size effects that gives rise to an increase of the relaxation

[†] Electronic Supplementary Information (ESI) available: [details of any supplementary information available should be included here]. See DOI: 10.1039/b000000x/

Centro de Ciências Naturais e Humanas, Universidade Federal do ABC, Av. dos Estados 5001, Santo André-SP, 09210-580, Brazil. Tel: +55 (11) 4996 0196; E-mail: herculano.martinho@ufabc.edu.br

time (Arrhenius behavior) as the temperature decreases. Thus, the crossover could not be associated to a FSC. In the second comment, Swenson *et al.*¹⁷ suggested the observed apparent transition at ~ 225 K is due to a confinement-induced vanishing of the α relaxation, thus the relaxation times obtained by Liu *et al.*¹³ at $T < 225$ K correspond to local relaxation process of supercooled confined water as proposed in a previous letter¹⁸.

A hydrophobically modified MCM-41-SA matrix was studied in the 200 – 300 K interval by Faraone¹⁴. No evidence of FSC was found corroborating others findings (see, e.g., ref.¹⁹) reporting that the dynamic crossover takes place at a much lower temperature in water confined in hydrophobic confining media. For water in double-wall carbon nanotubes the transition occurred at $T \sim 190$ K. The water's tetrahedral hydrogen-bond network rule in the low temperature dynamical properties of confined water has also been revealed. The hydration-level dependence of the single-particle dynamics of water confined in the ordered mesoporous silica MCM-41 measured by Bertrand *et al.*¹⁵ indicated that the dynamic crossover observed at full hydration was absent at monolayer hydration. The monolayer dynamics were significantly slower than those of water in a fully hydrated pore at ambient temperatures.

Two special dynamical transitions, apparently of universal character, were observed in biomolecules (see, e.g., refs.^{20–23}). The first transition occurred at $T_D \sim 180 - 220$ K and was observed in macromolecules with a hydration level $h > 0.18$. Pieces of evidence for dynamical crossover for hydration water in proteins and other biomolecules have also been shown (see, e.g., the review of Mallamace *et al.*²⁴). Mallamace *et al.*²⁴ concluded that the FSC is a general phenomenon that does not take place only in confined water. Their statement was based on experimental and computer simulation results on FSC observed in water in different physical conditions (bulk water, water in solutions and confined water). Based on the quasi-elastic neutron scattering measurements for lysozyme, Chen *et al.*²⁵ interpreted the transition at T_D as a FSC, where structured water makes a transition from a HDL to a LDL based on possible existence of LLCP⁴. However, Doster *et al.*²³ showed no evidence of such a FSC characteristic at T_D for in fully deuterated C-phycoerythrin protein. Recently, Wang *et al.*²⁶ observed the dynamic crossover for lysozyme with hydration level greater than the correspondent monolayer hydration level (i.e., $h = 0.30$ and $h = 0.45$). The authors observed the activation energies present weak hydration level and environmental dependencies, indicating local-like motion.

Thus, there are a lack of consensus about the occurrence of second critical point, the Widom line, and FSC of water. To obtain evidence regarding the existence of the liquid-liquid phase transition in deeply supercooled water, we present results concerning the water confined in micro/nanotubes of L-

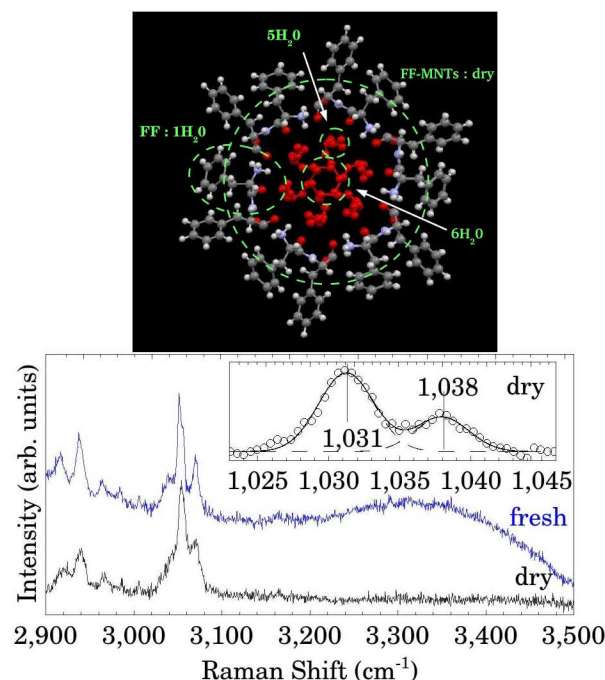


Fig. 1 (color online) *Top*: Core motif of FF-MNTs formed by six molecules of diphenylalanine (FF) arranged in a hexagonal pack, as seen from the a and b axes of the crystallographic unity cell. *Bottom*: Raman spectra for fresh and dry FF-MNTs samples. The inset shows the vibrational mode of benzene rings deconvoluted to two peaks at 1,031 and 1,038 cm^{-1} . This doublet structure is due to FF:water interaction.

diphenylalanine (FF-MNTs).

2 Materials and Methods

The FF-MNTs system is suitable for confining water in a controlled way. It can self-assemble into stiff, as well as chemically and thermally stable assemblies in aqueous solutions. X-ray analysis have show that FF-MNTs monomers crystallize with hydrogen-bonded head-to-tail chains in the form of helices with six dipeptide molecules per turn (top side of Fig. 1) and a channel core with a diameter of ~ 10 Å, that is filled with water molecules²⁷. Spectroscopic methods are powerful tools for exploring structural and dynamical properties of water¹². Raman spectroscopy is of special interest due to its high sensitivity and molecular specificity. This technique was employed to probe the microscopic dynamics of water inside FF-MNTs in the temperature interval of $10 < T < 290$ K. Each spectrum was deconvoluted to Pseudo-Voigt lineshape using the Fityk software²⁸. The full width half maximum (Γ) and maximum frequencies (ω_0) were computed for the vibrational modes of interest at each temperature. More details concerning sample

preparation (liquid phase strategy, described by Reches and Gazit²⁹) and Raman spectroscopy measurements were given in the Supplementary Information section.

Raman scattering can be used to probe the amount of water molecules in FF-MNTs via the linear dependence of the Raman mode position at the low-frequency side of the double-peak mode at $\sim 1,034 \text{ cm}^{-1}$ (vibrational mode of benzene rings) on water molecule number bonded to each diphenylalanine (FF) molecule³⁰. As could be observed in the inset of the bottom side of Fig. 1 the frequency of this mode was $1,031 \text{ cm}^{-1}$ in FF-MNTs sample confirming the pentamer water arrangements near FF in the structure (see Fig. 7 of ref.³⁰). The bottom side of Fig.1 shows the Raman spectra of fresh (immediately after the liquid phase reaction of preparation) and high-vacuum dried FF-MNTs sample. The OH-stretching vibration region between $3,200$ and $3,500 \text{ cm}^{-1}$ is an useful spectral window to probe bulk water presence. This broad vibrational region disappeared under drying process indicating that only confined water inside FF-MNTs is present in the sample.

The vibrational assignment was based on *first-principle* vibrational calculations^{31–36}. More details were described in the Supplementary Information section. The employed approach enabled us to obtain directly the contributions of each isolated water cluster to the Raman spectra. Due to the strong anharmonicity of the studied system, many vibrational modes corresponded to the calculated superposition of two or three eigenmodes.

3 Results and discussion

The temperature dependence ($10 - 290 \text{ K}$) of the low wavenumber ($20 - 150 \text{ cm}^{-1}$) Raman spectra of FF-MNTs is shown on Fig.2. The spectral variation above $T \sim 200 \text{ K}$ in the spectral window below 136 cm^{-1} is noteworthy. Almost all phonons in this regions broaden and soften on heating. Also, modes at $36; 45; 50; 60; 82;$ and 113 cm^{-1} experienced a noticeable intensity increasing. The detailed temperature dependence of the 82 cm^{-1} and 113 cm^{-1} bands will be discussed on following. Our vibrational assignment (see Supplementary Information section) indicated that the 82 cm^{-1} mode corresponds to an acceptor bend of water dimer³⁷ which links the pentamer and hexamer water clusters. The 113 cm^{-1} is a water pentamer torsion mode. Both modes are exclusive water vibrations.

The left scale of Fig.3a) and b) shows $\omega_0(T)$ for 82 and 113 cm^{-1} modes, respectively. Both presented a smooth softening on heating as result of crystal lattice thermal expansion without signature of structural phase transition²². Notwithstanding $\Gamma(T)$ displayed a clear anomaly close to $T \sim 200 \text{ K}$ for both modes (right scale of Fig.3a and 3b). Increasing temperature $\Gamma(T)$ increases indicating shorter phonon relaxation

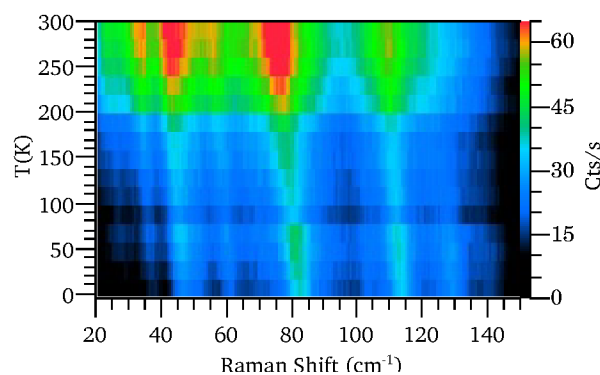


Fig. 2 (color online) Temperature dependence of the Raman spectra in the low frequency region.

time at high temperatures. The typical $\Gamma = 10 \text{ cm}^{-1}$ observed in FF-MNTs corresponds to relaxation time of $\sim 0.5 \text{ ps}$.

The mechanisms by which phonon in solid can be scattered are anharmonic Umklapp process including boundary, phonon-impurity, electron-phonon, or phonon-phonon scatterings³⁸. Each of these mechanism is associated with relaxation time which is inversely proportional to their relaxation rate. The total relaxation rate of phonon is given by Matthiessens rule $\tau^{-1} = \sum_i \tau_i^{-1}$. Usually the temperature dependence of optical phonons is dominated by phonon-phonon anharmonic decay³⁹. The two-phonon decay process behavior for $\Gamma(T)$ expected for 82 and 113 cm^{-1} phonons (following eq. 3.4 of ref.³⁹) is shown on Fig. 3. One could conclude that these phonons were only weakly damped by anharmonic interactions since $\Gamma(T) \ll \Gamma_{two-ph}$. Thus the two-phonon processes contributed only to a constant linewidth at $T \rightarrow 0$ limit. One

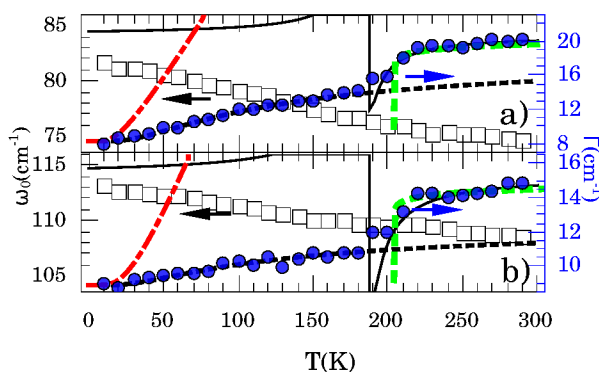


Fig. 3 (color online) Temperature dependency of ω_0 (left scale) and Γ (right scale, blue) for vibration modes at 82 cm^{-1} (a) and 113 cm^{-1} (b). The dash-dotted (red), solid (black), short-dashed (black), and dashed (green) lines are fit to two-phonon decay, non-Arrhenius (eq. 1), Arrhenius (eq. 2), and MCT (eq.4) expressions, respectively. The fitting parameters are indicated in the text.

possible reason is the absence of acoustic or optical phonons in the dispersion relation to match the conservation energy requirement. Thus, others possible decay channels could be explored.

The relaxation behavior of a deeply supercooled liquid is generally described by the viscosity-related main relaxation process (α -kind) and one or several secondary relaxation processes (β -kind). For α processes τ_α usually displays some degree of non-Arrhenius (or fragile) temperature dependence⁴⁰ being well-described by the Vogel-Fulcher-Tamman (VTF) law. The phonon relaxation rate in this case will be:

$$\Gamma_{fragile} = \Gamma_{two-ph} (1 + e^{-\frac{BT_0}{T-T_0}}) \quad (1)$$

where Γ_{two-ph} is a constant related to the residual two-phonon anharmonic decay, B is a constant that provides a measure of fragility and T_0 is the ideal glass transition temperature. The strong (or Arrhenius) temperature dependence will be

$$\Gamma_{strong} = \Gamma_{two-ph} (1 + e^{-\frac{E_A}{k_B T}}) \quad (2)$$

where E_A is the activation energy for the relaxation process and k_B is the Boltzmann constant.

The FSC is considered as a signature of the fluid crossing the Widom line. To investigate the structural relaxation mechanisms in FF-MNTs $\Gamma(T)$ experimental data were fitted to eqs. 1 and 2 as shown in left scale of Fig.3. Below $T \sim 200$ K the data for both modes were well-described by the strong behavior becoming fragile above this crossover temperature. The best parameters found fitting data to eqs. 1 and 2 were $E_A = 0.214$ kcal/mol, $B = 0.0478$, $T_0 = 187$ K. Γ_0 was fixed to $\Gamma_0 = \lim_{T \rightarrow 0} \Gamma(T)$.

The crossover temperature T_W was obtained from the expression⁴¹

$$\frac{1}{T_W} = \frac{1}{T_0} - \frac{Bk_B}{E_A} \quad (3)$$

and found to be $T_W = 204$ K.

The dynamic anomaly of viscosity and the structural relaxation time in water have often been explained with mode-coupling theory (MCT)⁴²⁻⁴⁴. MCT predicts that relaxation proceeds in essentially two steps in glass forming liquids at high temperatures ($T \gg T_c$) a fast (β) relaxation step and a slow (α) relaxation step. The latter is the primary relaxation and correlates to the temperature variation of shear viscosity. According to MCT the β process is temperature independent for $T > T_c$. The α relaxation characteristic time τ_α follows the critical temperature behavior⁴⁵ $\tau_\alpha \propto (T/T_c - 1)^{-\gamma}$ where γ is the critical exponent. Thus, the linewidth have a critical behavior:

$$\Gamma_{MCT}(T) = \Gamma_\beta + A(T/T_c - 1)^\gamma \quad (4)$$

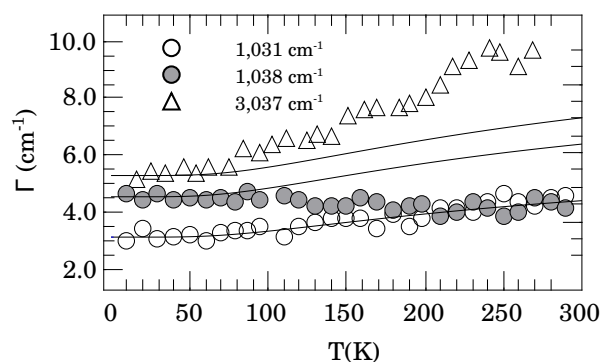


Fig. 4 $\Gamma(T)$ for 1,031 (open circles)/ 1,038 (closed circles) cm^{-1} benzene rings vibrational mode doublet and 3,037 (open diamond) cm^{-1} N-H stretching. The solid and dashed lines are the Arrhenius fit to the experimental data. The vertical line indicates $T_W = 204$ K.

with T_c the critical temperature that marks the changes from a regime where relaxation process are mastered by breaking and reforming the cages to a regime where the cages are frozen and diffusion is attained through hopping⁴⁶. It corresponds to the glassy transition temperature within this theory framework. We will test the previsions of MCT theory associating T_c to T_W . The dashed (green) lines in Figs. 3a) and b) show $\Gamma(T > T_W)$ for 82 cm^{-1} and 113 cm^{-1} bands data fitted to eq. 4 for 82 cm^{-1} and 113 cm^{-1} bands. The agreement was perfect above $1.05T_W$ for both data and furnished $\gamma = 0.054$ for the critical exponent. This value is exactly that predicted by the self-consistent approximation of MCT^{47,48}. It is important to notice that $\gamma = 0.070$ whether one considers vertex corrections⁴⁹. However, we notice that the fragile VTF model (eq. 1) presented a better accordance to the data close to the transition point.

Kumar, Franzese and Stanley⁵⁰ predicted that the dynamical crossover observed in cell model of water is independent of the presence of a LLCP being also present in a singularity-free scenario (SFS). In the SFS the dynamic crossover is interpreted as a consequence of a local breaking and reorientation of the bonds for the formation of new and more tetrahedrally oriented bonds. The work of Mazza *et al.*⁵¹ concerning the dynamics of hydration bond network of a percolating layer of water molecules in the first hydration shell of lysozyme at 0.3 g $\text{H}_2\text{O}/\text{g}$ protein interpreted the two dynamical crossovers observed at 252 K and 181 K for this sample as originated from fluctuations in the hydrogen bond (HB) formation and HB reordering network, respectively. These findings give strong support to the predictions presented by Kumar, Franzese and Stanley.

A timely comparison between these findings and our results need to be presented. The first question that need be addressed concern how the peptide backbone participates in

the crossover observed at 204 K. There are HB fluctuations propagating to FF structure? The possibility of HB fluctuations in FF-MNTs could be checked studying the temperature dependence of the $\sim 1,034 \text{ cm}^{-1}$ band. This band is composed of two subpeaks (at $1,031$ and $1,038 \text{ cm}^{-1}$ in our case) with the separation determined by the interaction between water and FF molecules via HB³⁰. Water weakly bonded to FF molecules in the nanochannel cores gives rise to the observed splitting. The $3,037 \text{ cm}^{-1}$ N-H stretching mode is another example of FF structural mode weakly coupled to HB which could be probed with the above-cited purpose. The data are presented on Fig.4. We notice that the $1,031 \text{ cm}^{-1}$ doublet counterpart presented Arrhenius behavior in the 10 – 290 K temperature interval. The high wavenumber $1,038 \text{ cm}^{-1}$ doublet counterpart presented an almost constant behavior. The N-H stretching mode appeared to relax slowly than Arrhenius law. Thus, no evidence of crossover was detected for these modes.

These results indicates that the dynamics of water confined in the nanochannel of FF-MNTs is almost isolated from the peptide backbone. Thus, HB fluctuations will be irrelevant in this case and surface or contact effects as well. We argue that the effects reported in FF-MNTs are directly correlated to the emergence of the LLCP probed in the isolated confined water clusters. The SFS does not applies in our case.

4 Conclusions

To the best of our knowledge, this is the first study of isolated dynamics of a specific geometry of water cluster (pentamer) in supercooled confined regime. We showed that the supercooled confined water in FF-MNTs exhibit a FSC at 204 K. From our analysis we concluded that this temperature corresponds to the Widom temperature T_W which supports the theory of Poole *et al.*⁴ in which there is a liquid-liquid transition to supercooled water and that it ends at a critical point. The divergence behavior of $\Gamma(T)$ at T_W furnished a critical exponent of $\gamma = 0.54$ in perfect agreement with that predicted by MCT without vertex corrections. Our analysis indicated that the non-local α -relaxation process dominate above $1.05T_W$. It was presented evidence concerning the irrelevant role of HB fluctuations for this system. Our results are consistent with the emergence of a second critical point of water in this system at $T_W = 204 \text{ K}$.

Acknowledgments The authors are grateful to the Brazilian agencies FAPESP, CAPES, and CNPq for financial support and to the Multiuser Central Facilities of UFABC for experimental support.

References

1 P. F. McMillan and H. E. Stanley, *Nature Physics*, 2010, **6**, 479–480.

- 2 X.-q. Chu, A. Faraone, C. Kim, E. Fratini, P. Baglioni, J. B. Leao and S.-H. Chen, *J. Phys. Chem. B*, 2009, **113**, 5001–5006.
- 3 D. Frenkel, *Physica A*, 2002, **313**, 1–31.
- 4 P. H. Poole, F. Sciortino, U. Essmann and H. E. Stanley, *Nature*, 1992, **360**, 324–328.
- 5 V. Holten and M. A. Anisimov, *Sci. Rep.*, 2012, **2**, 1–7.
- 6 P. Kumar, K. T. Wikfeldt, D. Schlesinger, L. G. Pettersson and H. E. Stanley, *Sci. Rep.*, 2013, **3**, 1–7.
- 7 P. Gallo, D. Corradini and M. Rovere, *J. Chem. Phys.*, 2013, **139**, 204503.
- 8 K. Ito, C. T. Moynihan and C. A. Angell, *Nature*, 1999, **398**, 492–495.
- 9 P. Gallo and M. Rovere, *The J. Chem. Phys.*, 2012, **137**, 164503.
- 10 A. Faraone, L. Liu, C.-Y. Mou, C.-W. Yen and S.-H. Chen, *J. Chem. Phys.*, 2004, **121**, 10843–10846.
- 11 S.-H. Chen, F. Mallamace, C.-Y. Mou, M. Broccio, C. Corsaro, A. Faraone and L. Liu, *P. Natl. Acad. Sci. USA*, 2006, **103**, 12974–12978.
- 12 F. Mallamace, M. Broccio, C. Corsaro, A. Faraone, D. Majolino, V. Venuti, L. Liu, C.-Y. Mou and S.-H. Chen, *P. Natl. Acad. Sci. USA*, 2007, **104**, 424–428.
- 13 L. Liu, S.-H. Chen, A. Faraone, C.-W. Yen and C.-Y. Mou, *Phys. Rev. Lett.*, 2005, **95**, 117802.
- 14 A. Faraone, K.-H. Liu, C.-Y. Mou, Y. Zhang and S.-H. Chen, *J. Chem. Phys.*, 2009, **130**, 134512.
- 15 C. E. Bertrand, Y. Zhang and S.-H. Chen, *Phys. Chem. Chem. Phys.*, 2013, **15**, 721–745.
- 16 S. Cervený, J. Colmenero and A. Alegria, *Phys. Rev. Lett.*, 2006, **97**, 189802.
- 17 J. Swenson, *Phys. Rev. Lett.*, 2006, **97**, 189801.
- 18 J. Swenson, H. Jansson and R. Bergman, *Phys. Rev. Lett.*, 2006, **96**, 247802.
- 19 X.-Q. Chu, A. I. Kolesnikov, A. P. Moravsky, V. Garcia-Sakai and S.-H. Chen, *Phys. Rev. E*, 2007, **76**, 021505.
- 20 T. Lima, M. Ishikawa and H. Martinho, *Phys. Rev. E*, 2014, **89**, 022715.
- 21 A. C. Fogarty, E. Duboué-Dijon, F. Sterpone, J. T. Hynes and D. Laage, *Chem. Soc. Rev.*, 2013, **42**, 5672–5683.
- 22 T. Lima, E. Sato, E. Martins, P. Homem-de Mello, A. Lago, M. Coutinho-Neto, F. Ferreira, C. Giles, M. Pires and H. Martinho, *J. Phys. Cond. Matt.*, 2012, **24**, 195104.
- 23 W. Doster, S. Busch, A. M. Gaspar, M.-S. Appavou, J. Wuttke and H. Scheer, *Phys. Rev. Lett.*, 2010, **104**, 098101.
- 24 F. Mallamace, C. Corsaro, P. Baglioni, E. Fratini and S.-H. Chen, *J. Phys. Cond. Matt.*, 2012, **24**, 064103.
- 25 S.-H. Chen, L. Liu, E. Fratini, P. Baglioni, A. Faraone and E. Mamontov, *Proc. Natl. Acad. Sci. U.S.A.*, 2006, **103**, 9012–9016.
- 26 Z. Wang, E. Fratini, M. Li, P. Le, E. Mamontov, P. Baglioni and S.-H. Chen, *Phys. Rev. E*, 2014, **90**, 042705.
- 27 M. Wang, S. Xiong, X. Wu and P. K. Chu, *Small*, 2011, **7**, 2801–2807.
- 28 M. Wojdyr, *J. Appl. Crystallogr.*, 2010, **43**, 1126–1128.
- 29 M. Reches and E. Gazit, *Science*, 2003, **300**, 625–627.
- 30 X. Wu, S. Xiong, M. Wang, J. Shen and P. K. Chu, *J. Phys. Chem. C*, 2012, **116**, 9793–9799.
- 31 P. Hohenberg and W. Kohn, *Phys. Rev.*, 1964, **136**, B864.
- 32 W. Kohn and L. J. Sham, *Phys. Rev.*, 1965, **140**, A1133.
- 33 CPMD, <http://www.cpmd.org/>, Copyright IBM Corp 1990-2008, Copyright MPI für Festkörperforschung Stuttgart., 1997-2001.
- 34 C. Lee, W. Yang and R. G. Parr, *Phys. Rev. B*, 1988, **37**, 785.
- 35 O. A. von Lilienfeld, I. Tavernelli, U. Rothlisberger and D. Sebastiani, *Phys. Rev. B*, 2005, **71**, 195119.
- 36 I.-C. Lin, M. D. Coutinho-Neto, C. Felsenheimer, O. A. von Lilienfeld, I. Tavernelli and U. Rothlisberger, *Phys. Rev. B*, 2007, **75**, 205131.
- 37 S. S. Xantheas and T. H. Dunning Jr, *J. Chem. Phys.*, 1993, **99**, 8774–8792.
- 38 M. T. Dove, in *Introduction to lattice dynamics*, Cambridge university

- press, 1993, vol. 4, ch. 8.
- 39 M. Balkanski, R. Wallis and E. Haro, *Phys. Rev. B*, 1983, **28**, 1928.
- 40 K. Grzybowska, M. Paluch, A. Grzybowski, S. Pawlus, S. Ancherbak, D. Prevosto and S. Capaccioli, *J. Phys. Chem. Lett.*, 2010, **1**, 1170–1175.
- 41 F. Mallamace, C. Branca, M. Broccio, C. Corsaro, N. Gonzalez-Segredo, J. Spooren, H. E. Stanley and S.-H. Chen, *Eur. Phys. J. Spec. Top.*, 2008, **161**, 19–33.
- 42 P. G. Debenedetti, *Metastable liquids: concepts and principles*, Princeton University Press, 1996.
- 43 F. W. Starr, F. Sciortino and H. E. Stanley, *Phys. Rev. E*, 1999, **60**, 6757–6768.
- 44 H. Tanaka, *J. Phys. Cond. Matt.*, 2003, **15**, L703.
- 45 A. Sokolov, J. Hurst and D. Quitmann, *Phys. Rev. B*, 1995, **51**, 12865.
- 46 P. Gallo and M. Rovere, *J. Chem. Phys.*, 2012, **137**, 164503.
- 47 J. Bhattacharjee, F. RA and B. RS, *Phys. Rev. A*, 1981, **24**, 1469–1475.
- 48 T. Ohta and K. Kawasaki, *Progr. Theo. Phys.*, 1976, **55**, 1384–1395.
- 49 F. Garisto and R. Kapral, *Phys. Rev. A*, 1976, **14**, 884–885.
- 50 P. Kumar, G. Franzese and H. E. Stanley, *Phys. Rev. Lett.*, 2008, **100**, 105701.
- 51 M. G. Mazza, K. Stokely, S. E. Pagnotta, F. Bruni, H. E. Stanley and G. Franzese, *P. Natl. Acad. Sci. USA*, 2011, **108**, 19873–19878.